Supporting Information

Asymmetrical Hole/Electron Transport in Donor-Acceptor Mixed-Stack Cocrystals

Ryonosuke Sato, Tadashi Kawamoto and Takehiko Mori

Single crystal structures

The diffraction data of (3T)(TCNQ), (4T)(TCNQ), and (4T)(F_4TCNQ) were collected by a Rigaku four-circle diffractometer (AFC-7R) with graphite-monochromatized Mo$K\alpha$ radiation (λ = 0.71069 Å). The X-ray oscillation photographs of (4T)(F_2TCNQ) were taken using a RIGAKU R-AXIS RAPID II imaging plate with Cu$K\alpha$ radiation from a rotation anode source with a confocal multilayer X-ray mirror (RIGAKU VM-Spider, λ = 1.54187 Å). The structures were solved by the direct method (SHELXT) and refined by the full-matrix least-squares method by applying anisotropic temperature factors for all non-hydrogen atoms using the SHELXL programs.[S1,S2]

The crystal data are listed in Table S1. Crystal structure of (3T)(TCNQ) has been previously solved under the assumption of $P2_1/n$, in which the 3T molecule is located on an inversion center.[50] The 3T molecule has two possible orientations (Fig. S1(b)). We can solve the structure with the space group of *C2*/*m*. Here, 3T is located on a *2*/*m* position. A 3T molecule has a two-fold axis, but the mirror plane makes two possible orientations. Since two disordered orientations are seemingly intrinsic, in the present work, the crystal structure is solved assuming the space group of *C2*. The interplanar distance between the 3T and TCNQ molecules is 3.36 Å. The stacking axis is by 20° tilted from normal to the molecular planes.

Crystal qualities of (4T)(F_2TCNQ) and (4T)(F_4TCNQ) are not sufficient, but (4T)(F_2TCNQ) is isostructural to (4T)(TCNQ).[51] (4T)(F_4TCNQ) also has basically the same stacking structure as these complexes as well as (dimethyl-4T)(F_4TCNQ) (Table S1).[60] The *a* axis and lattice angles of (4T)(F_4TCNQ) are, however, considerably different from the others. The overlap modes (Figs. S1(d), (f), and (h)) are quite similar, but when the stacks are viewed along the same direction, the cells are significantly different (Figs. S1(c), (e), and (g)). This indicates that the column structures are basically the same, but the arrangements of the adjacent columns are meaningfully different in the F_4TCNQ complex. The 4T and TCNQ molecules are located on inversion centers without any disorder. The 4T and F_nTCNQ molecules are alternately stacked with interplanar distances of 3.37, 3.33, and 3.31 Å, respectively for n = 0, 2 and 4.

Table S1 Crystallographic data of F_nTCNQ complexes of 3T and 4T.

	(3T)(TCNQ)	(4T)(TCNQ)	(4T)(F_2TCNQ)	(4T)(F_4TCNQ)[a]
Formula	$C_{24}H_{12}N_4S_3$	$C_{28}H_{14}N_4S_4$	$C_{28}H_{12}F_2N_4S_4$	$C_{28}H_{10}F_4N_4S_4$
Formula weight	452.57	534.69	570.67	606.65
Crystal System	monoclinic	triclinic	triclinic	triclinic
Space Group	*C*2	*P*–1	*P*–1	*P*–1
Shape	black needle	black needle	black needle	black needle
a (Å)	10.970(5)	7.861(4)	7.9104(5)	9.092(5)
b (Å)	12.704(4)	8.890(3)	8.8995(6)	9.151(4)
c (Å)	7.754(3)	10.291(8)	10.3989(7)	10.403(6)
α(deg.)	90	109.60(4)	109.866(3)	90.88(5)
β(deg.)	101.29(3)	109.29(5)	109.641(3)	129.50(4)
γ(deg.)	90	98.00(4)	97.879(4)	104.63(4)
V (Å^3)	1059.7(7)	613.7(7)	621.80(7)	628.0(7)
ρ (g cm^{-3})	1.418	1.447	1.524	1.604
Z-value	2	1	1	1
T (K)	298	297	271	297
Total reflns.	1697	4191	6801	2801
Unique reflns.(R_{int})	1407 (0.0229)	3571 (0.0684)	2009 (0.0779)	2210 (0.0931)
R_1 [$F^2 > 2\sigma(F^2)$]	0.0431	0.0624	0.1030	0.0919
wR_2 [All reflns.]	0.1230	0.1952	0.3315	0.3090
GOF	0.975	0.999	1.096	1.037

[a] (4T)(F_4TCNQ) cell parameters are not the standard triclinic form to facilitate comparison with other 4T complexes. The standard triclinic form is as follows: *a*' = 8.400(5) Å, *b*' = 9.092(5) Å, *c*' = 9.151(4) Å, α' = 75.37(4) °, β' = 73.00(4) °, and γ' = 72.86(4) °, where $\boldsymbol{a} = -\boldsymbol{b}'$, $\boldsymbol{b} = \boldsymbol{c}'$, and $\boldsymbol{c} = \boldsymbol{b}'-\boldsymbol{a}'$ is the transformation matrix.

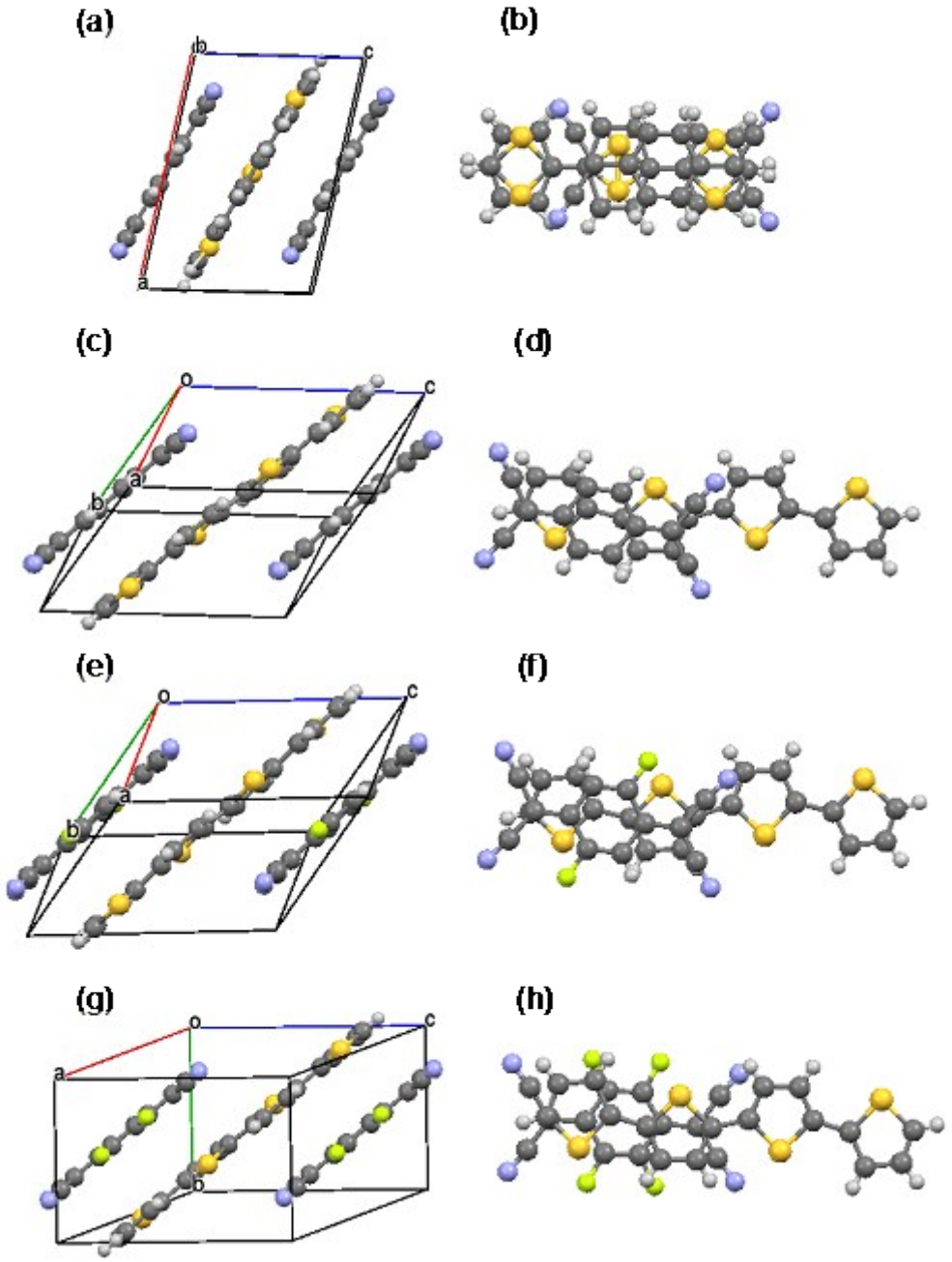

Fig. S1 (a) Mixed-stack column, and (b) donor-acceptor overlap in (3T)(TCNQ). (c) Mixed-stack column, and (d) donor-acceptor overlap in (4T)(TCNQ). (e) Mixed-stack column, and (f) donor-acceptor overlap in (4T)(F_2TCNQ). (g) Mixed-stack column, and (h) donor-acceptor overlap in (4T)(F_4TCNQ).

Degree of charge transfer

The charge transfer degrees ρ of the CT complexes were estimated from the bond lengths a ~ d and the C≡N stretching mode $\nu_{C\equiv N}$ of the TCNQ derivatives in the IR spectra as listed in Table S2 by using the following formula.[S3,S4]

$$\rho_{BL} = -26.28 + 27.94[(a + c)/(b + d)]$$

$$\nu_{C\equiv N} = 2227 - 44\rho_{IR}$$

Table S2 Bond lengths, the C≡N stretching mode, and the resulting ρ of the CT complexes.

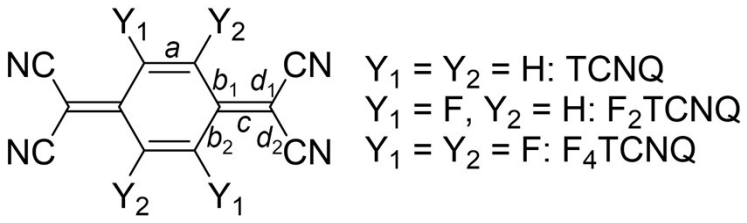

	(3T)(TCNQ)	(4T)(TCNQ)	(4T)(F_2TCNQ)	(4T)(F_4TCNQ)
a (Å) [a]	1.365/1.317	1.345	1.355	1.357
b (Å) [a]	1.475/1.400	1.434/1.435	1.443/1.425	1.441/1.414
c (Å)	1.388	1.388	1.378	1.383
d (Å) [a]	1.408/1.449	1.425/1.433	1.441/1.436	1.432/1.448
ρ_{BL}	0.32	0.39	0.30	0.42
$\nu_{C\equiv N}$ (cm^{-1})	2215.32	2215.32	2218.21	2219.18
ρ_{IR}	0.27	0.27	0.20	0.18

[a] For a, b and d, average of the two distances was used.

Cyclic Voltammetry (CV)

Redox potentials were measured by cyclic voltammetry (CV) on an ALS model 701E electrochemical analyzer using dry acetonitrile as a solvent and tetrabutylammonium hexafluorophosphate as an electrolyte. The working electrode was glassy carbon, and the counter electrode was platinum. Ag in a 0.01 M $AgNO_3$ solution was used as a reference electrode. The LUMO levels were estimated from the first half-wave reduction (F_nTCNQ) potentials by assuming the reference energy level of ferrocene/ferrocenium (Fc/Fc^+: $E^{1/2}$ = +0.195 V *vs*. $Ag/AgNO_3$ measured under the identical conditions) to be 4.8 eV from the vacuum level.[S5] These values are in excellent agreement with the reported values listed in the parentheses.[63,S6-S8]

Table S3 Redox potentials, and the energy levels.

	$E^{1/2}$ (V)	$E_{HOMO/LUMO}$ (eV)
3T	–	(–5.49)[63]
4T	–	(–5.41)[63]
TCNQ	–0.19	–4.61 (–4.60)[S6-S8]
F_2TCNQ	–0.01	–4.79 (–4.85)[S6-S8]
F_4TCNQ	0.18	–4.98 (–5.06)[S6-S8]

Partition method

In order to investigate signs of the different contributions, two bridge orbitals with the energies E_1 and E_2 are considered. The secular equation for the triad is as follows.

$$\begin{vmatrix} E_0 - E & t & t' & 0 \\ t & E_1 - E & 0 & t \\ t' & 0 & E_2 - E & t' \\ 0 & t & t' & E_0 - E \end{vmatrix} = 0 \qquad \text{(S1)}$$

The shift of the starting orbital energy, $E_0 - E$, in the first and fourth lines, is substituted by $2t^{eff}$. The diagonal terms, $E_i - E$, of the second and third lines are approximated by $E_i - E_0$ (i = 1 and 2), because $E_i - E$ is much larger than $2t^{eff}$. Then, this determinant is solved to give

$$t^{eff} = \frac{t^2}{E_1 - E_0} + \frac{t'^2}{E_2 - E_0}. \qquad \text{(S2)}$$

If the bridge orbital with energy E_2 has an opposite parity (Figure S1), we have to examine a secular equation with different signs of t'.

$$\begin{vmatrix} E_0 - E & t & t' & 0 \\ t & E_1 - E & 0 & t \\ t' & 0 & E_2 - E & -t' \\ 0 & t & -t' & E_0 - E \end{vmatrix} = 0 \qquad \text{(S3)}$$

This equation similarly affords the relation in which the first and second terms have opposite signs.

$$t^{eff} = \frac{t^2}{E_1 - E_0} - \frac{t'^2}{E_2 - E_0} \qquad \text{(S4)}$$

We can determine the signs from the parity of the bridge orbitals (Fig. S2). In addition, the sign changes depending on the sign of the denominator.

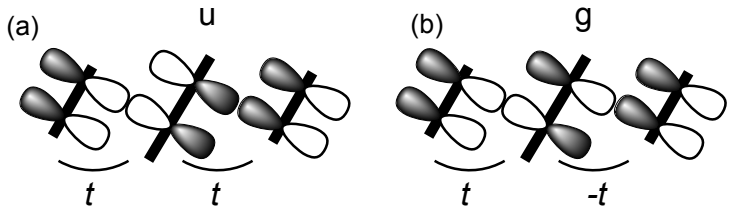

Fig. S2 Parity of bridge orbitals.

In order to confirm these relations, energy bands of the same situation are calculated. The energy band is obtained from the following secular equation.[59]

$$\begin{vmatrix} E_0 - E & 2t\cos ka & 2t'\cos ka \\ 2t\cos ka & E_1 - E & 0 \\ 2t'\cos ka & 0 & E_2 - E \end{vmatrix} = 0 \qquad \text{(S5)}$$

$E_1 - E$ and $E_2 - E$ are respectively approximated by $E_1 - E_0$ and $E_2 - E_0$ to give

$$E_0 - E = \left(\frac{4t^2}{E_1 - E_0} + \frac{4t'^2}{E_2 - E_0} \right) \cos^2 ka = 2\left(\frac{t^2}{E_1 - E_0} + \frac{t'^2}{E_2 - E_0} \right) \cos 2ka + \text{const.} \qquad \text{(S6)}$$

so that t^{eff} is given by eqn (S2). An example of the energy band is shown in Fig. S3(a). When the red band is regarded as TCNQ LUMO band, the bandwidth $4t^{eff}$ is determined by the transfer to the donor bridge orbitals. The calculated bandwidth (0.34 eV) is slightly smaller than the expectation from eqn (S2) (0.53 eV) because $E_i - E$ is not approximated to be $E_i - E_0$ in the band calculation.

When the two bridge orbitals have different kinds of parity,

$$\begin{vmatrix} E_0 - E & 2t\cos ka & 2t'i\sin ka \\ 2t\cos ka & E_1 - E & 0 \\ -2t'i\sin ka & 0 & E_2 - E \end{vmatrix} = 0 \qquad \text{(S7)}$$

gives

$$E_0 - E = \frac{4t^2}{E_1 - E_0}\cos^2 ka + \frac{4t'^2}{E_2 - E_0}\sin^2 ka$$

$$= 2\left(\frac{t^2}{E_1 - E_0} - \frac{t'^2}{E_2 - E_0}\right)\cos 2ka + \text{const.} \qquad \text{(S8)}$$

so eqn (S4) affords the bandwidth. The energy band in Fig. S3(b) represents the case of entire cancellation due to the same magnitude of even and odd parity transfers.

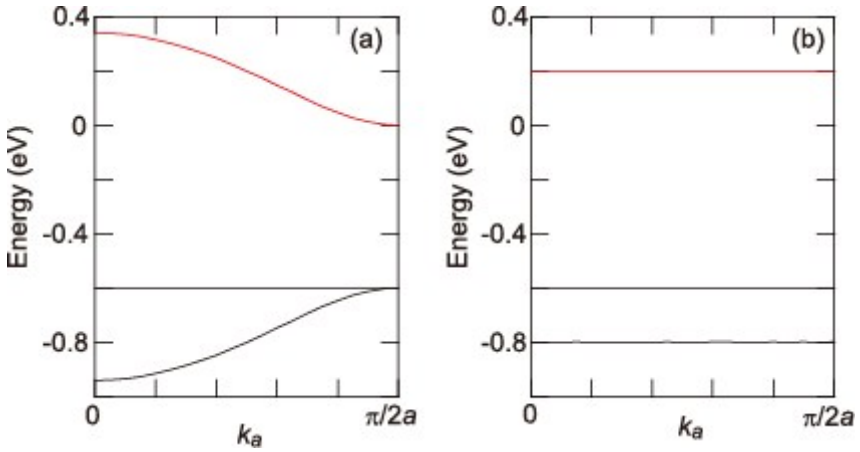

Fig. S3 Tight-binding energy band with two bridge orbitals with (a) even, and (b) odd parity. Parameters are $E_0 = 0$, $E_1 = E_2 = -0.6$ eV, and $t = t' = 0.2$ eV.

Energy levels of (4T)(TCNQ) monomers, dimers, and trimers are depicted in Fig. S4. In the complexes, D levels shift downward and A levels shift upward reflecting the charge transfer, and the D H/A L gap becomes 1 ~ 2 eV. The shift is regarded as approximately parallel. In the present partition calculations, $E_i - E_0$ is taken from the ADA triad energy levels.

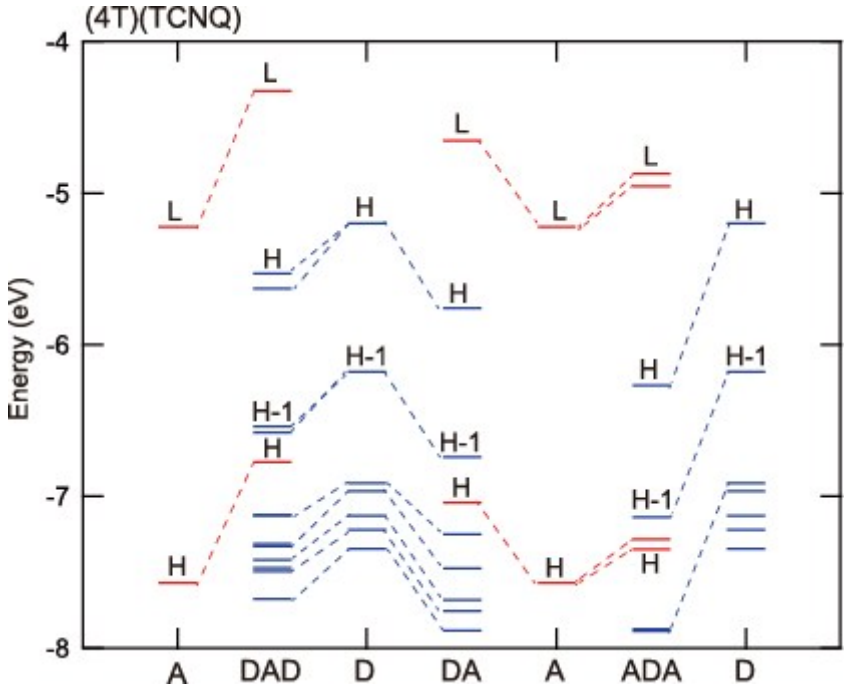

Fig. S4 Energy levels of (4T)(TCNQ) monomers, dimer, and trimers.

The partition calculations are listed in Tables S4 to S10. In (tetracene)(TCNQ), practically a single bridge orbital participates in the conduction: D H−1 for electrons and A H−1 for holes (Table S4). Electron conduction through D H−4 is by one order smaller than the H−1 conduction. In m-(tetracene)(TCNQ), several transfers are exactly zero owing to the symmetry, but the situation is not much different in t-(tetracene) (TCNQ) and (tetracene)(F_4TCNQ).

(Anthracene)(TCNQ) is in the same situation (Table S5), but the H/L interaction increases with lowering the temperature. Interestingly, t_h^{eff} once increases at 155 K, but decreases at 100

K (Table 2); this is in agreement with the observation of hole transport at the intermediate temperatures, but restoration of electron conduction at 100 K.[42] This happens due to the cancellation of the A L and H−1 contributions at 100 K (Table S5).

The results of (chrysene)(TCNQ) are in basic agreement with Ref. 45 (Table S6). For hole conduction, the L and H−1 pathways cancel each other. In (coronene)(TCNQ) and (coronene)(F_4TCNQ), two sets of molecular orbitals, H/H−1 and H−1/H−2, are approximately degenerate. Due to the cancellation between H−1 and H−3, the obtained t_e^{eff} is small (Table S6), but if this mechanism does not work, electron conduction is much more dominant.

In (BTBT)(F_nTCNQ), (DMeOBTBT)(F_nTCNQ), and (DBPP)(DMTCNQ), the H−1 conduction is overwhelmingly important, and these complexes show electron conduction (Table S7).

The H/L interaction is most important in (DBTTF)(TCNQ) and (DBPP)(DMDCNQI), and these complexes exhibit ambipolar properties (Table S8).

In (4T)(F_nTCNQ), the H−1 transfer is as large as the H/L transfer (Table S9) because the H−1 transfer also has stripe symmetry (Fig. 5). These two orbitals have different parity and cancel the electron transport so that the hole transport is larger than the electron transport. This mechanism is less important in (f*n*T)(TCNQ), and these complexes are more close to the ambipolar transport. In (DPTTA)(F_nTCNQ), hole transport is larger than electron transport due to the cancellation of the H and H−3 contributions for electron transport. Including (DP-P2P)(CyhNDI), these complexes are essentially ambipolar, though electron/hole dominance is derived from the sensitive balance of the bridge orbitals.

Table S4 Energy difference, transfers, and contributions to superexchange transfers (meV) in the partition calculation of (tetracene)(F_nTCNQ).

(a) m-(tetracene)(TCNQ)

Electron				Hole			
A L→	$E_i - E_0$	t	$t^2/(E_i - E_0)$	D H→	$E_i - E_0$	t	$t^2/(E_i - E_0)$
H	710	0	0	L	−710	0	0
H−1	2018	282	39	H	1639	0	0
H−2	2210	0	0	H−1	3215	199	−12
H−3	3126	0	0				
H−4	3455	107	−3				
Total			36				−12

(b) t-(tetracene)(TCNQ)

Electron				Hole			
A L→	$E_i - E_0$	t	$t^2/(E_i - E_0)$	D H→	$E_i - E_0$	t	$t^2/(E_i - E_0)$
H	710	14	0	L	−710	14	0
H−1	2018	313	49	H	1639	51	2
H−2	2210	14	0	H−1	3215	221	−15
H−3	3126	34	0				
H−4	3455	113	−4				
Total			46				−13

(c) (tetracene)(F_4TCNQ)

Electron				Hole			
A L→	$E_i - E_0$	t	$t^2/(E_i - E_0)$	D H→	$E_i - E_0$	t	$t^2/(E_i - E_0)$
H	1122	99	9	L	−1122	99	9
H−1	2127	317	47	H	1117	60	3
H−2	2182	72	−2	H−1	1982	201	−20
H−3	2359	45	1				
H−4	2711	73	−2				
Total			52				−8

Table S5 Energy difference, transfers, and contributions to superexchange transfers (meV) in the partition calculation of (anthracene)(TCNQ).

(a) 300 K

Electron				Hole			
A L→	$E_i - E_0$	t	$t^2/(E_i - E_0)$	D H→	$E_i - E_0$	t	$t^2/(E_i - E_0)$
H	1305	0	0	L	−1305	0	0
H−1	2410	309	40	H	1044	0	0
H−2	2999	0	0	H−1	2620	271	−28
Total			40				−28

A L→	$E_i - E_0$	t	$t^2/(E_i - E_0)$	D H→	$E_i - E_0$	t	$t^2/(E_i - E_0)$
H	1305	50	2	L	−1305	50	2
H−1	2410	302	38	H	1044	15	0
H−2	2999	6	0	H−1	2620	283	−31
Total			40				−29

(b) 155 K

Electron				Hole			
A L→	$E_i - E_0$	t	$t^2/(E_i - E_0)$	D H→	$E_i - E_0$	t	$t^2/(E_i - E_0)$
H	1305	103	8	L	−1305	103	8
H−1	2410	322	43	H	1044	43	2
H−2	2999	35	0	H−1	2620	307	−36
Total			50				−26

A L→	$E_i - E_0$	t	$t^2/(E_i - E_0)$	D H→	$E_i - E_0$	t	$t^2/(E_i - E_0)$
H	1305	28	1	L	−1305	28	1
H−1	2410	338	48	H	1044	34	1
H−2	2999	33	0	H−1	2620	284	−29
Total			48				−27

(c) 100 K

Electron				Hole			
A L→	$E_i - E_0$	t	$t^2/(E_i - E_0)$	D H→	$E_i - E_0$	t	$t^2/(E_i - E_0)$
H	1305	158	19	L	−1305	158	19
H−1	2410	305	39	H	1044	50	2
H−2	2999	60	−1	H−1	2620	255	−25
Total			56				−3

A L→	$E_i - E_0$	t	$t^2/(E_i - E_0)$	D H→	$E_i - E_0$	t	$t^2/(E_i - E_0)$
H	1305	151	17	L	−1305	151	17
H−1	2410	297	37	H	1044	28	1
H−2	2999	45	−1	H−1	2620	273	−29
Total			53			1	−10

Table S6 Energy difference, transfers, and contributions to superexchange transfers (meV) in the partition calculation of (chrysene)(TCNQ) and (coronene)(F_nTCNQ).

(a) (chrysene)(TCNQ)

Electron				Hole			
A L→	$E_i - E_0$	t	$t^2/(E_i - E_0)$	D H→	$E_i - E_0$	t	$t^2/(E_i - E_0)$
L	−2414	97	4	L	−1481	84	5
H	1481	84	5	H	867	53	3
H−1	2105	351	59	H−1	2443	110	−5
H−2	2250	103	−5				
H−3	3142	132	−6				
Total			57				3

(b) (coronene)(TCNQ)

Electron				Hole			
A L→	$E_i - E_0$	t	$t^2/(E_i - E_0)$	D H→	$E_i - E_0$	t	$t^2/(E_i - E_0)$
L	−2134	38	1	L	−1515	3	0
H	1515	3	0	H	833	83	8
H−1	1627	286	50	H−1	2409	1	0
H−2	2179	38	−1				
H−3	2311	290	−36				
Total			14				8

(c) (coronene)(F_4TCNQ)

Electron				Hole			
A L→	$E_i - E_0$	t	$t^2/(E_i - E_0)$	D H→	$E_i - E_0$	t	$t^2/(E_i - E_0)$
L	−2330	31	0	L	−1319	134	14
H	1319	134	14	H	920	21	0
H−1	1404	285	58	H−1	1786	60	−2
H−2	2138	118	−7				
H−3	2267	323	−46				
Total			19				11

Table S7 Energy difference, transfers, and contributions to superexchange transfers (meV) in the partition calculation of (BTBT)(F_nTCNQ), (DMeOBTBT)(F_nTCNQ), and (DBPP)(DMTCNQ).

(a) (BTBT)(TCNQ)

Electron				Hole			
A L→	$E_i - E_0$	t	$t^2/(E_i - E_0)$	D H→	$E_i - E_0$	t	$t^2/(E_i - E_0)$
H	1568	15	0	L	−1568	15	0
H−1	2075	341	56	H	781	7	6
H−2	2312	63	−2	H−1	2356	45	−1
H−3	2420	146	−9				
Total			46				5

(b) (BTBT)(F_2TCNQ)

Electron				Hole			
A L→	$E_i - E_0$	t	$t^2/(E_i - E_0)$	D H→	$E_i - E_0$	t	$t^2/(E_i - E_0)$
H	1447	18	0	L	−1447	18	0
H−1	1929	349	63	H	889	43	2
H−2	2191	76	−3	H−1	2029	61	−2
H−3	2342	138	−8				
Total			53				0

(c) (BTBT)(F_4TCNQ)

Electron				Hole			
A L→	$E_i - E_0$	t	$t^2/(E_i - E_0)$	D H→	$E_i - E_0$	t	$t^2/(E_i - E_0)$
H	1403	14	0	L	−1403	14	0
H−1	1874	370	73	H	837	47	3
H−2	2215	78	−3	H−1	1702	33	−1
H−3	2345	164	−11				
Total			59				2

(d) (DMeOBTBT)(TCNQ)

Electron				Hole			
A L→	$E_i - E_0$	t	$t^2/(E_i - E_0)$	D H→	$E_i - E_0$	t	$t^2/(E_i - E_0)$
L	−1156	20	4	L	−1446	313	68
H	1446	313	68	H	902	140	22
H−1	1614	15	0	H−1	2478	96	−4
H−2	1946	117	−7				
Total			65				86

(e) (DMeOBTBT)(F_2TCNQ)

Electron				Hole			
A L→	$E_i - E_0$	t	$t^2/(E_i - E_0)$	D H→	$E_i - E_0$	t	$t^2/(E_i - E_0)$
H	1247	69	4	L	−1247	69	4
H−1	1558	328	69	H	886	68	5
H−2	1614	33	−1	H−1	2030	57	−2
H−3	2278	163	−12				
Total			60				7

(f) (DMeOBTBT)(F_4TCNQ)

Electron				Hole			
A L→	$E_i - E_0$	t	$t^2/(E_i - E_0)$	D H→	$E_i - E_0$	t	$t^2/(E_i - E_0)$
H	1142	44	2	L	−1142	44	2
H−1	1477	339	78	H	1098	53	3
H−2	1496	28	−1	H−1	1963	46	−1
H−3	2231	187	−16				
Total			63				3

(g) (DBPP)(DMTCNQ)

Electron				Hole			
A L→	$E_i - E_0$	t	$t^2/(E_i - E_0)$	D H→	$E_i - E_0$	t	$t^2/(E_i - E_0)$
H	1115	172	26	L	−1115	172	26
H−1	1840	319	55	H	987	28	1
H−2	2028	47	1	H−1	2066	139	−9
H−3	2090	194	−18				
Total			65				18

Table S8 Energy difference, transfers, and contributions to superexchange transfers (meV) in the partition calculation of (DBTTF)(TCNQ) and (DBPP)(DMDCNQI).

(a) (DBTTF)(TCNQ)

Electron				Hole			
A L→	$E_i - E_0$	t	$t^2/(E_i - E_0)$	D H→	$E_i - E_0$	t	$t^2/(E_i - E_0)$
L+1	−2482	81	3	L	−1059	205	40
L	−2089	0	0	H	2178	78	3
H	1059	205	40	H−1	2455	21	0
H−1	2762	17	0				
H−2	2847	72	−2				
H−3	2946	177	−10				
Total			30				42

(b) (DBPP)(DMDCNQI)

Electron				Hole			
A L→	$E_i - E_0$	t	$t^2/(E_i - E_0)$	D H→	$E_i - E_0$	t	$t^2/(E_i - E_0)$
H	1438	253	44	L	−1438	253	44
H−1	2003	263	34	H	1469	89	5
H−2	2647	18	0	H−1	2485	58	−1
H−3	2895	129	−6				
Total			73				48

Table S9 Energy difference, transfers, and contributions to superexchange transfers (meV) in the partition calculation of (4T)(F_nTCNQ), (DPTTA)(F_nTCNQ), (f*n*T)(TCNQ), and (DP-P2P)(CyhNDI).

(a) (4T)(TCNQ)

Electron				Hole			
A L→	$E_i - E_0$	t	$t^2/(E_i - E_0)$	D H→	$E_i - E_0$	t	$t^2/(E_i - E_0)$
H	1311	274	57	L	−1311	274	57
H−1	2183	293	−39	H	1014	68	5
H−2	2920	34	0	H−1	2655	113	−5
H−3	2933	88	−3				
Total			16				57

(b) (4T)(F_2TCNQ)

Electron				Hole			
A L→	$E_i - E_0$	t	$t^2/(E_i - E_0)$	D H→	$E_i - E_0$	t	$t^2/(E_i - E_0)$
H	1212	285	67	L	−1212	285	67
H−1	1907	277	−40	H	1120	43	2
H−2	2206	37	1	H−1	2264	14	0
H−3	2325	61	−2				
H−4	2843	89	3				
Total			29				69

(c) (4T)(F_4TCNQ)

Electron				Hole			
A L→	$E_i - E_0$	t	$t^2/(E_i - E_0)$	D H→	$E_i - E_0$	t	$t^2/(E_i - E_0)$
H	1119	280	70	L	−1119	280	70
H−1	1879	276	−40	H	1230	37	1
H−2	2131	11	0	H−1	2806	113	−5
H−3	2264	78	−3				
Total			27				67

(d) (DPTTA)(F_2TCNQ)

Electron				Hole			
A L→	$E_i - E_0$	t	$t^2/(E_i - E_0)$	D H→	$E_i - E_0$	t	$t^2/(E_i - E_0)$
H	1212	156	20	L	−1212	156	20
H−1	1907	42	1	H	1120	44	2
H−2	2206	3	0	H−1	2264	22	0
H−3	2325	169	−12				
Total			9				22

(e) (DPTTA)(F_4TCNQ)

Electron				Hole			
A L→	$E_i - E_0$	t	$t^2/(E_i - E_0)$	D H→	$E_i - E_0$	t	$t^2/(E_i - E_0)$
H	1119	136	16	L	−1119	136	16
H−1	1879	20	0	H	1121	28	1
H−2	2131	22	0	H−1	1986	16	0
H−3	2264	163	−12				
Total			5				17

(f) (f3T)(TCNQ)

Electron				Hole			
A L→	$E_i - E_0$	t	$t^2/(E_i - E_0)$	D H→	$E_i - E_0$	t	$t^2/(E_i - E_0)$
H	1715	205	25	L	−1715	205	25
H−1	1933	41	1	H	633	73	8
H−2	2229	124	−7	H−1	2209	59	−2
H−3	2421	91	3				
Total			22				31

(g) (f4T)(TCNQ)

Electron				Hole			
A L→	$E_i - E_0$	t	$t^2/(E_i - E_0)$	D H→	$E_i - E_0$	t	$t^2/(E_i - E_0)$
H	1643	344	72	L	−1643	344	72
H−1	1972	25	0	H	705	94	13
H−2	2279	132	−8	H−1	2281	79	−3
H−3	2428	51	1				
H−4	2694	129	−6				
Total			60				83

(h) (DP-P2P)(CyhNDI)

Electron				Hole			
A L→	$E_i - E_0$	t [a]	$t^2/(E_i - E_0)$	D H→	$E_i - E_0$	t [a]	$t^2/(E_i - E_0)$
L	−1527	132	2	L+1	−3568	49	2
		−24				145	
H	1931	−166	−2	L	−1931	−166	−2
		24				24	
H−1	2023	85	−12	H	1361	199	−1
		−292				9	
H−2	3114	92	−2	H−1	1686	−66	−16
		−63				−400	
Total			−14				−17

[a] Owing to the noncentrosymmetric molecules, two transfers are independent, and the contributions are given by $t_1 t_2/(E_i - E_0)$.

Table S10 Energy difference, transfers, and contributions to superexchange transfers (meV) in the partition calculation of PMDA complexes of tetracene and phenazine.

(a) (tetracene)(PMDA)

Electron				Hole			
A L→	$E_i - E_0$	t	$t^2/(E_i - E_0)$	D H→	$E_i - E_0$	t	$t^2/(E_i - E_0)$
H	1751	283	46	L	−1751	283	46
H−1	2877	13	0	H	2432	9	0
H−2	3216	6	0	H−1	2465	23	0
H−3	4074	319	25				
Total			71				45

(b) (phenazine)(PMDA)

Electron				Hole			
A L→	$E_i - E_0$	t	$t^2/(E_i - E_0)$	D H→	$E_i - E_0$	t	$t^2/(E_i - E_0)$
H	2747	233	20	L	−2747	233	20
H−1	3249	41	1	H	1442	120	10
H−2	3563	6	0	H−1	1552	57	2
H−3	3701	302	25				
Total			45				32

References

S1 G. M. Sheldrick, *Acta Crystallogr. A* 2015, **71**, 3.

S2 G. M. Sheldrick, *Acta Crystallogr. C* 2015, **71**, 3.

S3 T. C. Umland, S.Allie, T. Kuhlmann, P. Coppens, *J. Phys. Chem.* 1988, **92**, 6456.

S4 J. S. Chappell, A. N. Bloch, W. A. Bryden, M. Maxfield, T. O. Poehler, D. O. Cowan, *J. Am. Chem. Soc.* 1981, **103**, 2442.

S5 M. L. Tang, A. D. Reicharrdt, P. Wei, Z. Bao, *J. Am. Chem. Soc*. 2009, **131**, 5264.

S6 P. W. Kenny, T. H. Jozefiak, L. L. Miller, *J. Org. Chem*. 1988, **53**, 5007.

S7 H. Ikegami, C. H. Chong, H. Yamochi, G. Saito, *Mol. Cryst. Liq, Cryst*. 2002, **382**, 21.

S8 S. S. Pac, G. Saito, *J. Solid State Chem*. 2002, **168**, 486-496.